^{18}F-FDG PET/CT as a Potential Predictor of Lung Inflammation After Arc-Based Radiotherapy for Esophageal Cancer: A Pilot Study

Chen-Xiong Hsu
National Yang Ming Chiao Tung University
Kuan-Heng Lin
National Yang Ming Chiao Tung University
Pei-Wei Shueng
Far Eastern Memorial Hospital
Yen-Wen Wu
Far Eastern Memorial Hospital
Wei-Ta Tsai
National Yang Ming Chiao Tung University
Chiu-Han Chang
Far Eastern Memorial Hospital
Hui-Ju Tien
Far Eastern Memorial Hospital
Shan-Ying Wang
Far Eastern Memorial Hospital
Tung-Hsin Wu (tunghsinwu@nycu.edu.tw)
National Yang Ming Chiao Tung University https://orcid.org/0000-0002-0583-7921
Greta S. P. Mok
University of Macau

Research Article

Keywords: 18F-FDG, PET/CT, radiation pneumonitis, esophageal cancer, arc-based radiotherapy

Posted Date: November 16th, 2021

DOI: https://doi.org/10.21203/rs.3.rs-1029931/v1

Abstract

Purpose

Fluorine-18-fuorodeoxyglucose (^{18}F-FDG) positron emission tomography/computerized tomography (PET/CT) scan serves as a useful tool not only for tumor detection, radiotherapy (RT) target volume delineation but also for the assessment of the inflammatory changes in normal organs. Previously we proposed the volume-based algorithm (VBA) method to reduce low dose-volume of lung by improving the arc angle in dynamic arc-based RT. The aim of this study was to assess lung inflammation by integrating ^{18}F-FDG PET/CT with VBA before and after arc-based RT for esophageal cancer (EC).

Methods

Thirty EC patients underwent ^{18}F-FDG PET/CT imaging before RT (pre-RT) and after RT (post-RT) on a retrospective pilot study. The VBA was used to define the high dose (HD) (≧ 5 Gy) region and the low dose (LD) (< 5 Gy) region in the lungs. The maximum standardized uptake value (SUVmax), mean standardized uptake value (SUVmean), and global lung glycolysis (GLG) of the HD and LD regions in the lungs were quantified. The pre-RT and post-RT SUVmax, SUVmean, and GLG of HD and LD regions in lungs were analyzed in radiation pneumonitis (RP) ≧ grade 1 and non-radiation pneumonitis (nRP) lungs. The mean lung dose (MLD), V_5, V_{10}, V_{15}, V_{20}, V_{25}, V_{30} in lungs were analyzed. Vx indicates the organ volume percentage exceeding a radiation dose of x (Gy). Receiver-operating characteristic curves were used to identify optimal cut-off values for RP after RT.

Results

In RP lungs (n = 30), the SUVmax, SUVmean and GLG of the HD region between pre-RT and post-RT showed significant increases (all $p < 0.05$). Whereas there were no significant differences in those of the HD and LD regions in nRP lungs (n = 22). The post-RT SUVmax (2.78 vs. 2.07, $p = 0.000$) and post-RT SUVmean (0.64 vs. 0.52, $p = 0.015$) of the HD region in RP lungs were significantly higher than those in nRP lungs. The MLD (10.15 Gy vs. 8.11 Gy, $p = 0.041$), lung V_5 (49.78% vs. 38.07%, $p = 0.010$) and lung V_{10} (32.25% vs. 24.71%, $p = 0.017$) in the RP lungs were significantly higher than those in nRP lungs. The area under the curve (AUC) of post-RT SUVmax of the HD regions was 0.852, and the AUC of the lung V_5 was 0.727. For predicting RP, the optimal cut-off values of post-RT SUVmax and lung V_5 were > 2.28 and > 47.14%. respectively.

Conclusion

This study successfully integrated ^{18}F-FDG PET/CT with VBA to assess RP in EC patients undergoing dynamic arc-based RT. The post-RT SUVmax and post-RT SUVmean of HD (≧5 Gy) regions can be used to evaluate RP. The post-RT SUVmax > 2.28 of HD regions and lung V_5 > 47.14% may be a potential predictor of RP. ^{18}F-FDG PET/CT is a promising tool to detect RP for EC patients treated with arc-based RT.

Introduction

Functional and metabolic imaging with Fluorine-18-fuorodeoxyglucose (^{18}F-FDG) positron emission tomography/computed tomography (PET/CT) has been widely utilized to detect malignant tumor cells (1) and also to quantify the inflammation based on the metabolism of normal tissues (2, 3). Volume-based semi-quantitative parameters such as standardized uptake values (SUVs), metabolic tumor volume, and total lesion glycolysis could guide cancer diagnosis, staging, metastasis detection, and interpretation of treatment responses for esophageal cancer (EC) (4–6).

Radiation pneumonitis (RP), i.e., radiation-induced inflammation in the lung tissues, is one of the most common side effects after radiotherapy (RT) for EC (7, 8). Castillo et al. (9) and Hart et al. (10) indicated that the quantitative parameters of ^{18}F-FDG PET/CT could be used as indicators for detecting RP for EC patients. Abdulla et al. (11) combined the mean standardized uptake value (SUVmean) with the normal lung tissue volume to calculate the global lung glycolysis (GLG). They pointed out that GLG is a potential biomarker for detecting RP.

Several studies indicated that the incidence of RP has a highly linear relationship with the lung volume receiving low radiation dose (12, 13). Pinnix et al. (14) showed that lung V_5 > 55% could be used as a predictor for RP. Wang et al. (15) demonstrated that when lung $V_5 \leq 42\%$ the incidence of RP could drop to 3%. The lung V_5 is a crucial predictor of RP. To reduce the lung V_5, Chang et al. (16) designed the fan-shaped complete block to limit the beam angle while optimizing the RT plans in helical tomotherapy. Additionally, we proposed the volume-based algorithm (VBA) method to reduce lung V_5 by improving the arc angle in dynamic arc-based RT (17). Therefore, we aim to assess lung inflammation by integrating ^{18}F-FDG PET/CT with VBA before and after arc-based RT for EC.

Materials And Methods

Study population

Thirty EC patients treated with volumetric modulated arc therapy (VMAT) or tomotherapy between 2014 and 2018 were eligible for analysis. The ^{18}F-FDG PET/CT scans were acquired one week before RT (pre-RT) and one to three months after RT (post-RT). The patients were included with stage I to III according to the 7th AJCC TNM staging systems for EC (18). The study was approved by the Research Ethics Review Committee of Far Eastern Memorial Hospital (FEMH-IRB No.: 108069-E).

^{18} F-FDG PET/CT scans, quantification analysis, and evaluation of RP

PET/CT scans were acquired on a GE Discovery VCT PET/CT scanner (GE Medical Systems, Amersham, UK). Patients were required to fast for 6 hours before the PET/CT scan to achieve a blood glucose level of

<140 mg/dL. Patients were intravenously injected with ^{18}F-FDG according to their body weight (4 MBq/kg), and then rested for 60 minutes before image acquisition. CT images were acquired with the following parameters: tube voltage of 120 kVp, tube current with automatic exposure control from 10 to 300 mA, slice thickness of 3.75 mm, pitch of 1, and matrix size of 512 × 512. The scan range was from the top of head to mid-thigh. Three-dimensional PET images were acquired with the z-axis field-of-view (FOV) of 15 cm for 3 minutes at each bed position. PET images were reconstructed using Ordered Subset Expectation Maximization (OS-EM) algorithm, corrected for normalization, attenuation, random and scattered coincidences.

SUV is a semi-quantitative evaluation method used in PET. It mainly evaluates the ^{18}F-FDG uptake in tissues, organs, tumors, or regions of interest (ROI). The calculation method is as follows:

$$SUV = \frac{tissue\ \ concentration\ \ (MBq/mL)}{injected\ \ activity\ \ (mCi)/body\ \ weight\ \ (kg)}$$

Tissue concentration represents the tissue radioactivity per unit volume obtained after quantitative PET image reconstruction in the target FOV.

The maximum SUV (SUVmax) is defined as the maximum voxel value within the ROI; SUVmean is the average SUV value in all pixels within the ROI. The GLG could be obtained by multiplying the SUVmean and lung volume. It is a derivative of the total lesion glycolysis (TLG). TLG is a parameter for evaluating tumor activity and a prognostic factor of the tumor. TLG is focused on a lesion. In contrast, GLG is focused on lung. Several studies have used GLG to detect normal tissue inflammation (11, 19).

The calculation method is as follows:

$$GLG\ \ (cm^3) = SUVmean \times volume\ \ (cm^3)$$

According to the Common Terminology Criteria for Adverse Events 4.0 (20), RP was diagnosed through clinical symptoms and the radiographic changes on the CT scans of patients. RP (≧ grade 1) was interpreted by two experienced physicians at our institution.

Computed tomography simulation and radiation treatment planning

The CT simulation images were input into the Pinnacle treatment planning system (version 9.8, Philips Medical Systems North America, Andover, MA, USA) to design a RT plan. The clinical tumor volume (CTV) was designed to cover a region with subclinical disease from gross tumor volume (GTV) by expanding 4 cm superiorly and inferiorly, and 0.5 cm laterally on both sides, anteriorly and posteriorly. To define the planning target volume (PTV), organ movements caused by breathing, swallowing, and position uncertainty in each therapy were considered. The normal organs such as the heart, lungs, and spinal cord were defined. According to the size and shape of the tumor, different gantry arc angles were designed by

medical physicists. The prescribed dose to the PTV and the dose constraints of organs at risk were based on the International Commission on Radiation Units and Measurements Report 50 (ICRP 50) and esophageal and esophagogastric junction cancers, version 1.2015, NCCN Clinical Practice Guidelines in Oncology (21). The mean lung dose (MLD), V_5, V_{10}, V_{15}, V_{20}, V_{25}, V_{30} in lungs were collected. A dose-volume histogram parameter of Vx was defined as the percentage of the organ volume exceeding a radiation dose of x (Gy).

Image fusion and the high dose (HD) and the low dose (LD) regions segmentation

The PET images and the simulation CT images were fused using the MIM vista treatment planning system (version 6.8.4, MIM Software Inc., Cleveland, US). The images were adjusted and aligned based on the myocardium and spine. The Hounsfield unit (HU) between -950 HU and -250 HU was defined as lung volume on CT images (13), and region overlapping with the trachea and bronchus were manually removed. To avoid the ^{18}F-FDG uptake of the chest wall from affecting the calculation of metabolic response in the lung, the lung volume was obtained by shrinking a 1.5 mm thick slab inward from its original 3D boundary in simulation CT. Spill-out artifacts would appear in the ^{18}F-FDG high uptake area of the heart, liver, and lesion, which would affect the ^{18}F-FDG value in the adjacent regions (22). Therefore, the regions with SUV higher than 2.5 in the thoracic cavity were subtracted (23).

According to the VBA established by our team (17), we proposed the VBA method to reduce lung V5 in dynamic arc-based RT. Therefore, we integrated the irradiated lung volume in RT planning and volume-based parameters in PET/CT. We used the 5 Gy isodose curve to distinguish high dose (HD) (≧ 5 Gy) and low dose (LD) (< 5 Gy) regions in the lung volume (Fig. 1) to assess lung inflammatory changes pre- and post-RT. The SUVmean, SUVmax and GLG of HD and LD regions in the lungs were quantified in the pre- and post-RT PET/CT respectively.

Statistical analysis

The SPSS software package (version 24.0; IBM Corporation., Armonk, NY, USA) was used for statistical analysis. A two-tailed paired t-test was used to compare the metabolic response of the HD and LD regions between pre- and post-RT. An independent t-test was used to compare the metabolic response of the HD and LD regions as well as lung dose between RP and non-radiation pneumonitis (nRP) lungs. A $p < 0.05$ was considered statistically significant. Receiver operator characteristic (ROC) curves and area under the curves (AUCs) of metabolic response and lung dose were performed, and the optimal cut-off value was determined by the Youden index (24).

Results

Patient population

Thirty EC patients treated with VMAT were included between 2014 and 2018. The detailed patient characteristics were shown in Table 1. The median of the prescribed dose to PTV was 45 Gy. The median interval time between pre-RT ^{18}F-FDG PET/CT and RT was 17 days (range 12 - 29 days). The median interval time between RT and post-RT ^{18}F-FDG PET/CT was 37 days (range 21 - 89 days). The median interval time between the pre- and post-RT ^{18}F-FDG PET/CT scans was 68 days (range 98 - 174 days). Eleven patients were identified as nRP, and 19 patients were identified as RP (≥ grade 1). Twenty-two nRP lungs and 30 RP (≥ grade 1) lungs were identified. There were 14 right lungs and 16 left lungs with RP in 30 lungs.

Table 1
Patient characteristics

Characteristics	No. of Patients (n = 30)
Sex	
Male	20
Female	10
Age (years)	
Median	56
Range	43 – 78
Staging	
I	3
II	9
III	18
Chemotherapy	
Yes	30
No	0
RT technique	
VMAT	13
Tomotherapy	17
Prescription dose	
Median (Gy)	45
Range (Gy)	41 - 50.4
Interval time between RT and post-PET/CT	
Median (days)	37
Range (days)	21 – 89
nRP lungs	22
RP lungs (≥ grade 1)	30
Right lungs	14
Left lungs	16

Characteristics	No. of Patients (n = 30)
Both right and left lungs	11

RT, radiotherapy; RP, Radiation pneumonitis; nRP, non-radiation pneumonitis; VMAT, volumetric modulated arc therapy.

^{18}F-FDG PET metabolic response in lungs

Table 2 showed the metabolic response of the HD and LD regions in the right and left lungs between pre-RT and post-RT. There were significant increases in SUVmax, SUVmean, and GLG of the HD regions between pre-RT and post-RT. However, there were no significant differences in SUVmax, SUVmean, and GLG of the LD regions between pre-RT and post-RT.

Table 2
Comparison of the metabolic response in lungs between pre- and post- RT.

		Parameter	Pre-RT	Post-RT	Absolute change (Δ)	Relative change	Pre-RT vs. Post-RT *p*-value
Right lungs	HD region	SUVmax	2.04 ± 0.53	2.35 ± 0.72	0.30 ± 0.71	15 %	0.024*
(n = 30)		SUVmean	0.50 ± 0.10	0.56 ± 0.17	0.07 ± 0.14	13 %	0.034*
		GLG (cc)	300.79 ± 138.59	375.12 ± 181.42	77.47 ± 146.91	28 %	0.010*
	LD region	SUVmax	1.89 ± 0.47	1.89 ± 0.38	0.02 ± 0.40	1 %	0.918
		SUVmean	0.44 ± 0.09	0.47 ± 0.13	0.04 ± 0.11	8 %	0.136
		GLG (cc)	450.19 ± 185.51	457.23 ± 185.13	10.24 ± 153.65	2 %	0.806
Left lungs	HD region	SUVmax	2.02 ± 0.39	2.41 ± 0.50	0.39 ± 0.49	20 %	0.000*
(n = 30)		SUVmean	0.52 ± 0.11	0.59 ± 0.17	0.07 ± 0.13	12 %	0.013*
		GLG (cc)	317.39 ± 117.87	401.40 ± 184.85	85.02 ± 136.48	28 %	0.002*
	LD region	SUVmax	1.79 ± 0.48	1.96 ± 0.48	0.17 ± 0.57	10 %	0.119
		SUVmean	0.44 ± 0.09	0.47 ± 0.14	0.04 ± 0.11	9 %	0.082
		GLG (cc)	282.42 ± 130.87	283.36 ± 141.29	2.06 ± 89.51	1 %	0.955

Values were presented as mean ± SD

* $p<0.05$

RT, radiotherapy; HD, high dose; LD, low dose; SUV, standard uptake value; GLG, global lung glycolysis.

^{18} F-FDG PET metabolic response between RP and nRP lungs

Table 3 showed the metabolic response in RP and nRP lungs between pre- and post-RT. In RP lungs (n = 30) between pre-RT and post-RT SUVmax, SUVmean and GLG of the HD regions showed significant increases (all $p < 0.05$). However, there were no significant differences in the metabolic response of the HD and LD regions in nRP lungs.

Table 4 showed the post-RT metabolic response and the RT dose between RP and nRP lungs. The post-RT SUVmax (2.78 vs. 2.07, $p = 0.000$) and post-RT SUVmean (0.64 vs. 0.52, $p = 0.015$) of the HD regions in RP lungs were significantly higher than those of the HD regions in nRP lungs. However, there were no significant differences in the GLG of the HD regions between RP and nRP lungs. The MLD (10.15 Gy vs. 8.11 Gy, $p = 0.041$), lung V_5 (49.78% vs. 38.07%, $p = 0.010$) and lung V_{10} (32.25% vs. 24.71%, $p = 0.017$) of the RP lungs were significantly higher than those of nRP lungs.

Table 3
Comparison of the metabolic response in RP and nRP lungs between pre- and post-RT.

			Parameter	Pre-RT	Post-RT	*p*-value
RP lungs (n = 30)	Right lungs (n = 14)	HD region	SUVmax	2.10 ± 0.60	2.83 ± 0.79	0.002*
			SUVmean	0.52 ± 0.12	0.64 ± 0.21	0.040*
			GLG (cc)	314.98 ± 151.93	394.29 ± 206.68	0.044*
		LD region	SUVmax	2.01 ± 0.60	2.06 ± 0.44	0.721
			SUVmean	0.43 ± 0.10	0.51 ± 0.16	0.049*
			GLG (cc)	452.58 ± 202.19	500.59 ± 178.43	0.222
	Left lungs (n = 16)	HD region	SUVmax	2.05 ± 0.38	2.68 ± 0.52	0.000*
			SUVmean	0.51 ± 0.12	0.65 ± 0.20	0.001*
			GLG (cc)	348.26 ± 115.15	451.61 ± 207.45	0.020*
		LD region	SUVmax	1.77 ± 0.59	1.95 ± 0.55	0.319
			SUVmean	0.42 ± 0.11	0.51 ± 0.15	0.007*
			GLG (cc)	245.36 ± 131.97	289.99 ± 159.11	0.016*
nRP lungs (n = 22)	Right lungs (n = 11)	HD region	SUVmax	2.06 ± 0.47	2.02 ± 0.25	0.786
			SUVmean	0.51 ± 0.08	0.51 ± 0.10	0.921
			GLG (cc)	278.58 ± 123.79	344.58 ± 173.13	0.282
		LD region	SUVmax	1.79 ± 0.17	1.72 ± 0.20	0.451
			SUVmean	0.45 ± 0.07	0.44 ± 0.09	0.269
			GLG (cc)	483.64 ± 181.87	415.91 ± 188.39	0.206
	Left lungs (n = 11)	HD region	SUVmax	2.04 ± 0.44	2.12 ± 0.29	0.639
			SUVmean	0.55 ± 0.10	0.53 ± 0.10	0.246

		Parameter	Pre-RT	Post-RT	*p*-value
		GLG (cc)	266.64 ± 113.65	327.81 ± 141.17	0.115
	LD region	SUVmax	1.77 ± 0.30	1.97 ± 0.41	0.203
		SUVmean	0.45 ± 0.08	0.45 ± 0.10	0.759
		GLG (cc)	332.18 ± 113.09	279.59 ± 118.74	0.118

Values were presented as mean ± SD

* $p<0.05$

RT, radiotherapy; RP, radiation pneumonitis; nRP, non-radiation pneumonitis; HD, high dose region; LD, low dose region; SUV, standard uptake value; GLG, global lung glycolysis.

Table 4
Comparison of post-RT metabolic response and RT dose between RP and nRP lungs.

Parameter	RP lungs (n = 30)	nRP lungs (n = 22)	*p*-value
Post-RT metabolic response in HD region			
SUVmax	2.78 ± 0.64	2.07 ± 0.27	0.000*
SUVmean	0.64 ± 0.20	0.52 ± 0.10	0.015*
GLG (cc)	422.43 ± 204.77	336.26 ± 155.18	0.104
RT dose of lung			
Mean lung dose (Gy)	10.15 ± 3.88	8.11 ± 2.83	0.041*
V_5 (%)	49.78 ± 17.69	38.07 ± 11.86	0.010*
V_{10} (%)	32.25 ± 12.20	24.71 ± 8.80	0.017*
V_{15} (%)	22.38 ± 10.01	17.43 ± 7.81	0.060
V_{20} (%)	16.32 ± 8.47	13.24 ± 6.68	0.165
V_{25} (%)	12.49 ± 7.30	10.21 ± 5.69	0.230
V_{30} (%)	9.39 ± 6.10	7.73 ± 4.78	0.293

Values were presented as mean ± SD

Vx, percentage of the total organ volume exceeding a radiation dose of x (Gy)

* $p<0.05$

RT, radiotherapy; RP, radiation pneumonitis; nRP, non-radiation pneumonitis; HD, high dose region; SUV, standard uptake value; GLG, global lung glycolysis;

Roc Curve Analysis, Aucs, And Cut-off Values

The AUCs of post-RT SUVmax, post-RT SUVmean, and post-RT GLG of the HD regions were 0.852 (p = 0.000, 95% CI, 0.719-0.931), 0.667 (p = 0.025, 95% CI, 0.523-0.792), and 0.668 (p = 0.029, 95% CI, 0.524-0.793) respectively for discriminating the RP and nRP lungs (Fig. 2). The difference of areas in the AUC between post-RT SUVmax and post-RT SUVmean, post-RT SUVmax and post-RT GLG, and post-RT SUVmean and post-RT GLG were 0.179 (p = 0.020), 0.179 (p = 0.038), and 0.0007 (p = 0.993) respectively. An ROC analysis of RP demonstrated that the AUC for post-RT SUVmax was greater than those for post-RT SUVmean or post-RT GLG. Thus, the optimal cut-off value of post-RT SUVmax was 2.28 with 80.00% sensitivity and 86.36% specificity.

The AUCs of MLD, lung V_5, and lung V_{10} were 0.665 (p = 0.031, 95% CI, 0.521-0.790), 0.727 (p = 0.001, 95% CI, 0.586-0.841), and 0.711 (p = 0.003, 95% CI, 0.569-0.829) respectively for discriminating the RP and nRP lungs (Fig. 3). The difference of areas in the AUC between MLD and lung V_5, MLD and V_{10}, and lung V_5 and V_{10} were 0.062 (p = 0.070), 0.046 (p = 0.063) and 0.015 (p = 0.609) respectively. An ROC analysis of RP demonstrated that the AUC for lung V_5 was greater than those for MLD or lung V_{10}. The optimal cut-off value of lung V_5 was 47.14 with 60.00% sensitivity and 81.82% specificity.

Discussion

Increased ^{18}F-FDG uptake occurs not only in tumor cells with upregulated glucose transporter but also in the inflammatory process of normal tissue with cellular hypermetabolism (25). In recent years, several studies used ^{18}F-FDG PET/CT to assess and quantify the inflammation of lung tissue after RT for thoracic cancers (19, 26). Our study successfully assessed lung inflammation between HD and LD regions by integrating ^{18}F-FDG PET/CT with VBA in EC patients undergoing dynamic arc-based RT. We found that the SUVmax, SUVmean, and GLG increased significantly in the HD regions of RP lungs between pre- and post-RT. The present study indicated that post-RT SUVmax > 2.28 and the lung V_5 > 47.14% could be a predictor for RP.

Several studies demonstrated that ^{18}F-FDG PET/CT could be used to evaluate RP after RT (2, 27, 28). Yue et al. (22) found that the changes of SUVmax, SUVmean, and GLG in lungs could detect the severity of RP during the first 6 months after treatment. Abdulla et al. (11) indicated that SUVmean and GLG in lung parenchyma could be the potential biomarkers to quantify RP after thoracic RT in lung cancer. De Ruysscher et al. (29) found that the SUVmax highly correlated with clinical radiation-induced lung toxicity during the first week of thoracic RT. In the abovementioned studies, the analysis of VOIs was divided into the affected lung, the non-affected lung, or the global lung volume to measure the metabolic response. However, the non-affected lung would still receive low-dose radiation ≧ 5 Gy during RT for lung cancer and EC. Numerous studies reported that the lung V_5 might reach as high as 40 to 60% in EC, which indicated that 40 to 60% of the lung volume might receive absorbed doses ≧ 5 Gy. Low-dose radiation could be a significant predictor of RP (14, 15, 30). Based on the VBA (17), the present study used the 5 Gy isodose curve to distinguish HD (≧ 5 Gy) and LD (< 5 Gy) regions in the lung volume to assess the relationship between metabolic response and absorbed dose. There were statistically significant increases in the SUVmax, SUVmean, and GLG of HD regions between pre- and post-RT. Furthermore, we found that there were no statistically significant increases in the SUVmax, SUVmean, and GLG of LD regions between pre- and post-RT.

Researchers have found that radiation-induced lung inflammation after the lungs received higher radiation doses (13, 31). Radiographically evident changes are uncommon when the total radiation dose delivered is less than 30 Gy, but they are almost always seen with doses higher than 40 Gy (32, 33). Furthermore, Zhang et al. (34) showed that there was a significant difference in the SUVmean of the lungs between with or without RP group received more than 35 Gy for non-small cell lung cancer patients.

It should be noted that several studies had evaluated patients with symptomatic RP (≥ grade 2) and asymptomatic RP by using volume-based ^{18}F-FDG PET (22, 34). Yue et al. (22) found the cut-off value of SUVmax, SUVmean, and GLG were 4.54, 0.78, and 2295 after RT predicted later development of symptomatic RP (≥ grade 2). The present study found that there were significant differences between pre- and post-RT SUVmax, SUVmean, and GLG of the HD regions in the RP lungs. We found the optimal cut-off value of post-RT SUVmax, post-RT SUVmean, and post-RT GLG were 2.28, 0.56, and 287.65 for prediction of RP, respectively. The cut-off value of this study was lower than those of Yue et al. The main reason was probably that we aimed to detect asymptomatic RP (≥ grade 1) while they detected symptomatic RP (≥ grade 2). Therefore, the cut-off value might be more sensitive to detect asymptomatic RP. Our study showed that post-RT SUVmax with the highest AUC has a sensitivity of 80% and a specificity of 86.36%. The post-RT SUVmax > 2.28 could be used as an early predictor for RP with grade ≥ 1.

It is common to assess the relation between radiation absorbed dose and the risk of symptomatic RP. Graham et al. (35) indicated that the incidence of ≥ grade 2 RP was associated with the V_{20}. Tonison et al. (36) found that the lung V_{20} should be kept below 23% to decrease the incidence of symptomatic RP. Wang et al. (15) demonstrated that the lung V_5 was highly related to the risk of RP, and the risks of V_5 < 42% and V_5 > 42% causing RP within 1 year were 3% and 38%, respectively. Pinnix et al. (14) noted that a lung V_5 exceeding 55% was associated with the maximum likelihood ratio for RP. Jo et al. (37) showed a statistically significant association between the development of grade 2-3 RP and pulmonary dosimetric parameters, including lung V_5, V_{10}, V_{15}, V_{20}, V_{25} and MLD. The AUC value was highest for V_5. However, we evaluated changes of lung dose and metabolic response in patients with ≥ grade 1 RP versus nRP to detect the presence of RP at the earlier stage. The results of the present study revealed that there were significant differences between RP and nRP in the MLD, lung V_5, and lung V_{10}. However, there were no significant differences for lung V_{15}, V_{20}, and V_{25}. The lung V_5 has the highest AUC, with a sensitivity of 60.00% and specificity of 81.82% similar to the results of the previous study. We recommend limiting the V_5 to ≦ 47.14% to decrease the incidence of the ≥ grade 1 RP. Additionally, it was feasible to distinguish the HD and LD regions to assess RP by the 5 Gy isodose in our study.

There were some limitations in this study. First, this study was a retrospective pilot study, and we only analyzed the existing clinical data. Most EC patients did not regularly have ^{18}F-FDG PET/CT scans within 3 months after RT, which resulted in the relatively small sample size in this study. Second, the interval time between completion of RT and post-RT PET/CT scan ranged from 21 days to 89 days. The degree of metabolism may present in different stages of the inflammatory process. Third, the two PET/CT scans were performed before and after the RT treatment. Therefore, the lung volume might change in different PET/CT scans, somehow leading GLG to change. Last, the fusion and registration of simulation CT images and PET/CT images were based on the experience of the operators in this study. There might be some discordances in the manual operation. Therefore, further prospective studies with more patients are needed to verify our results.

Conclusion

This study successfully integrated ^{18}F-FDG PET/CT with VBA to assess RP in EC patients undergoing dynamic arc-based RT. The post-RT SUVmax and post-RT SUVmean of HD regions (≧5 Gy) can be used to evaluate RP. The post-RT SUVmax > 2.28 of HD regions and lung V_5 > 47.14% may be a potential predictor of RP. ^{18}F-FDG PET/CT is a promising tool to detect RP for EC patients treated with arc-based RT.

Abbreviations

18F-FDG: Fluorine-18-fuorodeoxyglucose; PET/CT: Positron emission tomography/computerized tomography; RT: Radiotherapy; VBA: Volume-based algorithm; EC: Esophageal cancer; Pre-RT: Before RT; Post-RT: After RT; HD: High dose; LD: Low dose; SUVmax: Maximum standardized uptake value; SUVmean: Mean standardized uptake value; GLG: Global lung glycolysis; RP: Radiation pneumonitis; nRP: Non-radiation pneumonitis; MLD: Mean lung dose; VMAT: Volumetric modulated arc therapy; FOV: Field-of-view; OS-EM: Ordered subset expectation maximization; ROI: Regions of interest; TLG: Total lesion glycolysis; CTV: Clinical tumor volume; GTV: Gross tumor volume; PTV: Planning target volume; ICRP 50: International Commission on Radiation Units and Measurements Report 50; HU: Hounsfield unit; ROC: Receiver operator characteristic; AUC: Area under the curves.

Declarations

Acknowledgements

Not applicable.

Author contributions

T.H. Wu and C.X. Hsu conceived and designed the research; H.J. Tien, C.H. Chang and S.Y. Wang performed the experiments; P.W. Shueng, Y.W. Wu, W.T. Tsai and T.H. Wu analyzed the data; K.H. Lin and C.X. Hsu wrote the procedure and prepared figures; K.H. Lin, C.X. Hsu and G.S.P. Mok wrote the main manuscript text. All authors approved the final manuscript

Funding

This work was partly supported by Ministry of Science and Technology, Taiwan (#MOST 109-2314-B-010-023-MY3), and National Yang Ming Chiao Tung University Far Eastern Memorial Hospital Joint Research Program (#NYCU-FEMH 105FN04 and 106DN02).

Availability of data and materials

The datasets used and/or analyzed during the current study are available from the corresponding author on reasonable request.

Ethics approval

The institutional review board of Far Eastern Memorial Hospital (No. 108069-E) approved this retrospective study and waived the need for written informed consent.

Consent for publication

Not applicable.

Conflict of interest

The authors declare no competing interests.

Author details

[1]Department of Biomedical Imaging and Radiological Sciences, National Yang Ming Chiao Tung University, Taipei, Taiwan. [2]Division of Radiation Oncology, Far Eastern Memorial Hospital, New Taipei City, Taiwan. [3]Industrial Ph.D. Program of Biomedical Science and Engineering, National Yang Ming Chiao Tung University, Taipei, Taiwan. [4]Faculty of Medicine, School of Medicine, National Yang Ming Chiao Tung University, Taipei, Taiwan. [5]Department of Nuclear Medicine, Far Eastern Memorial Hospital, New Taipei City, Taiwan. [6]Division of Cardiology, Cardiovascular Medical Center, Far Eastern Memorial Hospital, New Taipei City, Taiwan. [7]Biomedical Imaging Laboratory, Department of Electrical and Computer Engineering, Faculty of Science and Technology, University of Macau, Macau, SAR, China

References

1. Ben-Haim S, Ell P. ^{18}F-FDG PET and PET/CT in the Evaluation of Cancer Treatment Response. Journal of Nuclear Medicine. 2009;50(1):88–99.
2. Stumpe KD, Dazzi H, Schaffner A, von Schulthess GK. Infection imaging using whole-body FDG-PET. European journal of nuclear medicine. 2000;27(7):822–32.
3. Mok GS, Choi FP, Chu WC. Actinomycosis imitating parotid cancer with metastatic lymph nodes in FDG PET/CT. Clinical nuclear medicine. 2011;36(4):309–10.
4. Pennathur A, Gibson MK, Jobe BA, Luketich JD. Oesophageal carcinoma. The Lancet. 2013;381(9864):400–12.
5. Schreurs LMA, Janssens ACJW, Groen H, Fockens P, van Dullemen HM, van Berge Henegouwen MI, et al. Value of EUS in Determining Curative Resectability in Reference to CT and FDG-PET: The Optimal Sequence in Preoperative Staging of Esophageal Cancer? Annals of Surgical Oncology. 2016;23(5):1021–8.
6. Han S, Kim YJ, Woo S, Suh CH, Lee JJ. Prognostic Value of Volumetric Parameters of Pretreatment 18F-FDG PET/CT in Esophageal Cancer: A Systematic Review and Meta-analysis. Clinical nuclear medicine. 2018;43(12):887–94.

7. Jain V, Berman AT. Radiation Pneumonitis: Old Problem, New Tricks. Cancers (Basel). 2018;10(7).
8. Cui Z, Tian Y, He B, Li H, Li D, Liu J, et al. Associated factors of radiation pneumonitis induced by precise radiotherapy in 186 elderly patients with esophageal cancer. Int J Clin Exp Med. 2015;8(9):16646–51.
9. Castillo R, Pham N, Castillo E, Aso-Gonzalez S, Ansari S, Hobbs B, et al. Pre–Radiation Therapy Fluorine 18 Fluorodeoxyglucose PET Helps Identify Patients with Esophageal Cancer at High Risk for Radiation Pneumonitis. 2015;275(3):822–31.
10. Hart JP, McCurdy MR, Ezhil M, Wei W, Khan M, Luo D, et al. Radiation pneumonitis: correlation of toxicity with pulmonary metabolic radiation response. Int J Radiat Oncol Biol Phys. 2008;71(4):967–71.
11. Abdulla S, Salavati A, Saboury B, Basu S, Torigian DA, Alavi A. Quantitative assessment of global lung inflammation following radiation therapy using FDG PET/CT: a pilot study. European journal of nuclear medicine and molecular imaging. 2014;41(2):350–6.
12. Tanabe S, Myojin M, Shimizu S, Fujino M, Takahashi H, Shirato H, et al. Dose-volume analysis for respiratory toxicity in intrathoracic esophageal cancer patients treated with definitive chemoradiotherapy using extended fields. J Radiat Res. 2013;54(6):1085–94.
13. Guerrero T, Johnson V, Hart J, Pan T, Khan M, Luo D, et al. Radiation pneumonitis: local dose versus [18F]-fluorodeoxyglucose uptake response in irradiated lung. Int J Radiat Oncol Biol Phys. 2007;68(4):1030–5.
14. Pinnix CC, Smith GL, Milgrom S, Osborne EM, Reddy JP, Akhtari M, et al. Predictors of radiation pneumonitis in patients receiving intensity modulated radiation therapy for Hodgkin and non-Hodgkin lymphoma. Int J Radiat Oncol Biol Phys. 2015;92(1):175–82.
15. Wang S, Liao Z, Wei X, Liu HH, Tucker SL, Hu CS, et al. Analysis of clinical and dosimetric factors associated with treatment-related pneumonitis (TRP) in patients with non-small-cell lung cancer (NSCLC) treated with concurrent chemotherapy and three-dimensional conformal radiotherapy (3D-CRT). Int J Radiat Oncol Biol Phys. 2006;66(5):1399–407.
16. Chang C-H, Mok G, Shueng P-W, Yeh H-P, Shiau A-C, Tien H-J, et al. Fan-Shaped Complete Block on Helical Tomotherapy for Esophageal Cancer: A Phantom Study. BioMed research international. 2015;2015:959504.
17. Lin K-H, Hsu C-X, Wang S-Y, Mok GSP, Chang C-H, Tien H-J, et al. Volume-based algorithm of lung dose optimization in novel dynamic arc radiotherapy for esophageal cancer. Sci Rep. 2021;11(1):4360.
18. Rice TW, Blackstone EH, Rusch VW. 7th Edition of the AJCC Cancer Staging Manual: Esophagus and Esophagogastric Junction. Annals of Surgical Oncology. 2010;17(7):1721–4.
19. Jahangiri P, Pournazari K, Torigian DA, Werner TJ, Swisher-McClure S, Simone CB, 2nd, et al. A prospective study of the feasibility of FDG-PET/CT imaging to quantify radiation-induced lung inflammation in locally advanced non-small cell lung cancer patients receiving proton or photon radiotherapy. European journal of nuclear medicine and molecular imaging. 2019;46(1):206–16.

20. National Cancer Institute NIoH, US Department of Health and Human Services.. Common Terminology Criteria for Adverse Events (CTCAE), Version 4.0. NIH publication 09-7473. Published May 29, 2009; Revised June 14, 2010. http://evs.nci.nih.gov/ftp1/CTCAE/CTCAE_4.03_2010-06-14_QuickReference_5x7.pdf. Accessed March 16, 2015.
21. Ajani JA, D'Amico TA, Almhanna K, Bentrem DJ, Besh S, Chao J, et al. Esophageal and esophagogastric junction cancers, version 1.2015. J Natl Compr Canc Netw. 2015;13(2):194–227.
22. Yue J, McKeever M, Sio TT, Xu T, Huo J, Shi Q, et al. Association of lung fluorodeoxyglucose uptake with radiation pneumonitis after concurrent chemoradiation for non-small cell lung cancer. Clinical and translational radiation oncology. 2017;4:1–7.
23. Hong JH, Kim HH, Han EJ, Byun JH, Jang HS, Choi EK, et al. Total Lesion Glycolysis Using (1)(8)F-FDG PET/CT as a Prognostic Factor for Locally Advanced Esophageal Cancer. J Korean Med Sci. 2016;31(1):39–46.
24. Youden WJ. Index for rating diagnostic tests. Cancer. 1950;3(1):32–5.
25. Metser U, Even-Sapir E. Increased (18)F-fluorodeoxyglucose uptake in benign, nonphysiologic lesions found on whole-body positron emission tomography/computed tomography (PET/CT): accumulated data from four years of experience with PET/CT. Seminars in nuclear medicine. 2007;37(3):206–22.
26. Torigian D, Dam V, Chen X, Saboury B, Udupa J, Rashid A, et al. In vivo quantification of pulmonary inflammation in relation to emphysema severity via partial volume corrected18F-FDG-PET using computer-assisted analysis of diagnostic chest CT. Hellenic journal of nuclear medicine. 2013;16.
27. Petit SF, van Elmpt WJ, Oberije CJ, Vegt E, Dingemans AM, Lambin P, et al. [¹⁸F] fluorodeoxyglucose uptake patterns in lung before radiotherapy identify areas more susceptible to radiation-induced lung toxicity in non-small-cell lung cancer patients. Int J Radiat Oncol Biol Phys. 2011;81(3):698–705.
28. Hicks RJ, Mac Manus MP, Matthews JP, Hogg A, Binns D, Rischin D, et al. Early FDG-PET imaging after radical radiotherapy for non-small-cell lung cancer: inflammatory changes in normal tissues correlate with tumor response and do not confound therapeutic response evaluation. Int J Radiat Oncol Biol Phys. 2004;60(2):412–8.
29. De Ruysscher D, Houben A, Aerts HJ, Dehing C, Wanders R, Ollers M, et al. Increased (18)F-deoxyglucose uptake in the lung during the first weeks of radiotherapy is correlated with subsequent Radiation-Induced Lung Toxicity (RILT): a prospective pilot study. Radiother Oncol. 2009;91(3):415–20.
30. Wang L, Li C, Meng X, Li C, Sun X, Shang D, et al. Dosimetric and Radiobiological Comparison of External Beam Radiotherapy Using Simultaneous Integrated Boost Technique for Esophageal Cancer in Different Location. Frontiers in oncology. 2019;9:674-.
31. McCurdy MR, Castillo R, Martinez J, Al Hallack MN, Lichter J, Zouain N, et al. [18F]-FDG uptake dose–response correlates with radiation pneumonitis in lung cancer patients. Radiotherapy and Oncology. 2012;104(1):52–7.
32. Libshitz HI, Southard ME. Complications of radiation therapy: the thorax. Seminars in roentgenology. 1974;9(1):41–9.

33. Marks LB, Spencer DP, Bentel GC, Ray SK, Sherouse GW, Sontag MR, et al. The utility of SPECT lung perfusion scans in minimizing and assessing the physiologic consequences of thoracic irradiation. International Journal of Radiation Oncology*Biology*Physics. 1993;26(4):659–68.
34. Zhang Y, Yu Y, Yu J, Fu Z, Liu T, Guo S. 18FDG PET–CT standardized uptake value for the prediction of radiation pneumonitis in patients with lung cancer receiving radiotherapy. Oncol Lett. 2015;10(5):2909–14.
35. Graham MV, Purdy JA, Emami B, Harms W, Bosch W, Lockett MA, et al. Clinical dose-volume histogram analysis for pneumonitis after 3D treatment for non-small cell lung cancer (NSCLC). Int J Radiat Oncol Biol Phys. 1999;45(2):323–9.
36. Tonison JJ, Fischer SG, Viehrig M, Welz S, Boeke S, Zwirner K, et al. Radiation Pneumonitis after Intensity-Modulated Radiotherapy for Esophageal Cancer: Institutional Data and a Systematic Review. Sci Rep. 2019;9(1):2255-.
37. Jo I-Y, Kay C-S, Kim J-Y, Son S-H, Kang Y-N, Jung J-Y, et al. Significance of low-dose radiation distribution in development of radiation pneumonitis after helical-tomotherapy-based hypofractionated radiotherapy for pulmonary metastases. Journal of Radiation Research. 2013;55(1):105–12.

Figures

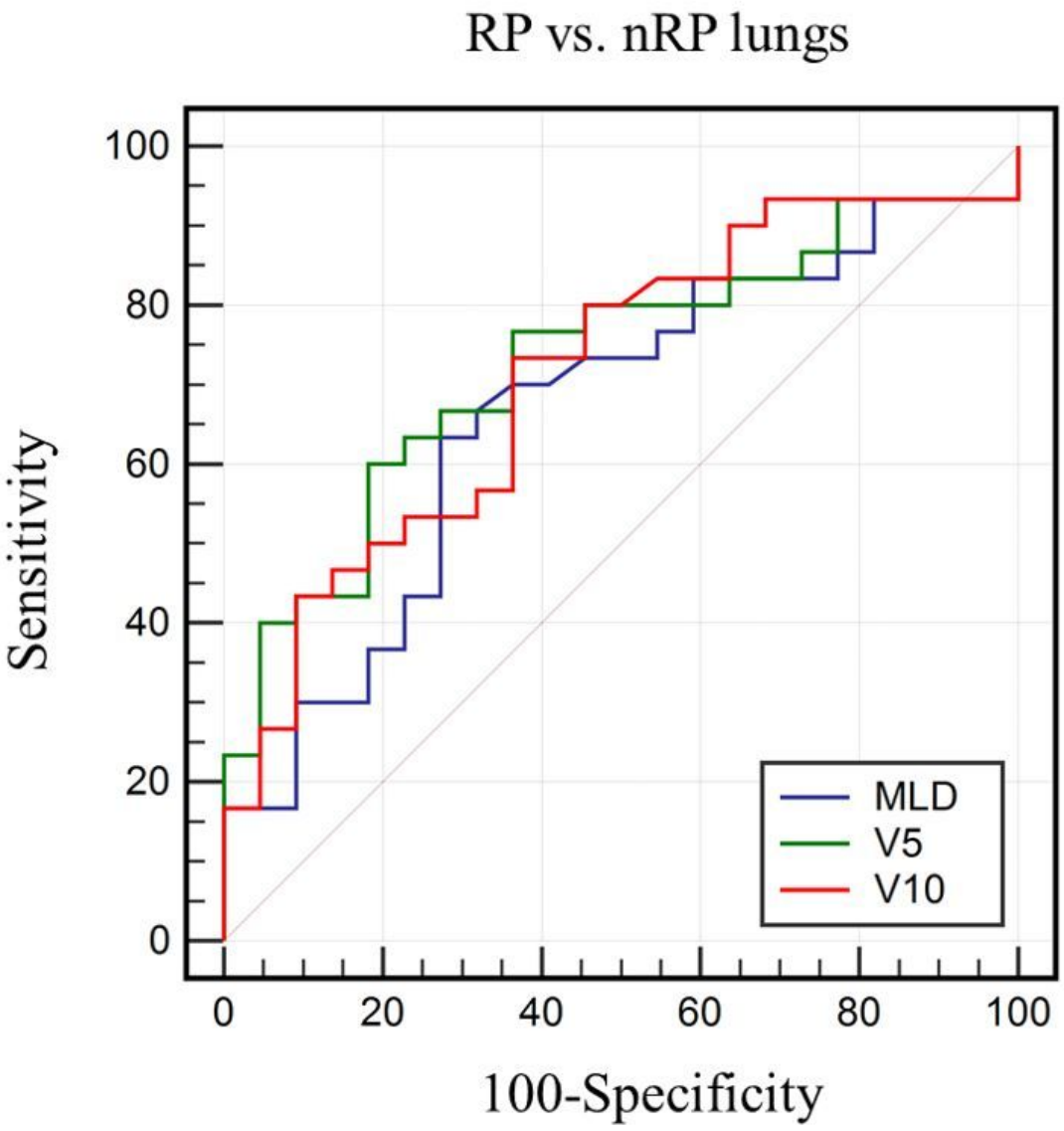

Figure 1

(A) Pre-RT PET/CT image fused with 5 Gy isodose curve; (B) simulation CT with isodose curves (5-50 Gy); (C) post-RT PET/CT image fused with 5 Gy isodose curve. The yellow line is 5 Gy isodose curve. The blue line is the right HD region. The red line is the left HD region. The brown line is the right LD region. The green line is left LD region. The pink line is GTV. The SUVmean, SUVmax and GLG of HD and LD regions in the lungs were quantified in the pre- and post-RT PET/CT respectively.

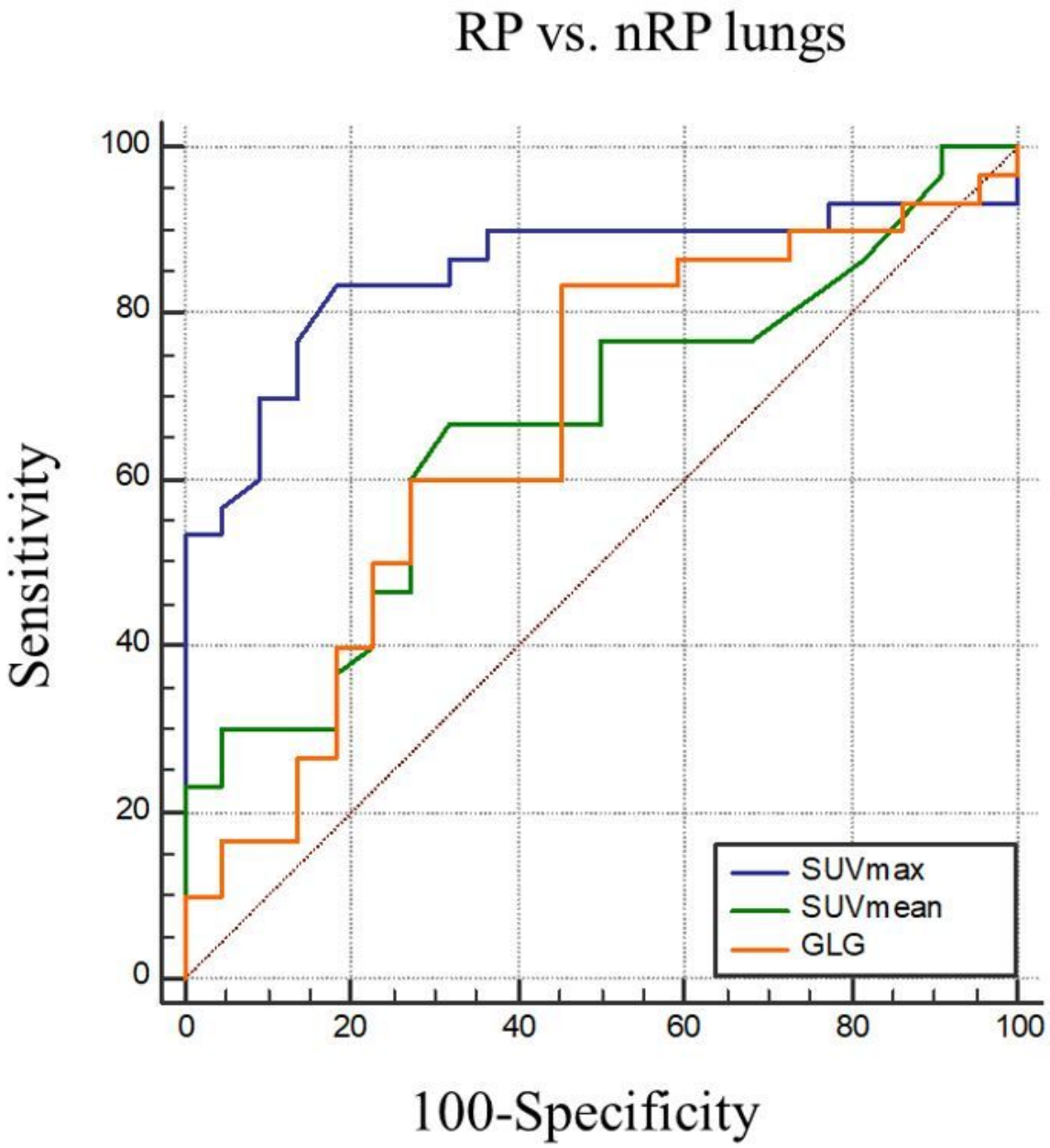

Figure 2

Comparison of area under the receiver operating characteristic curve of post-RT SUVmax, post-RT SUVmean, and post-RT GLG of high dose (HD) regions for discriminating the RP and nRP lungs.

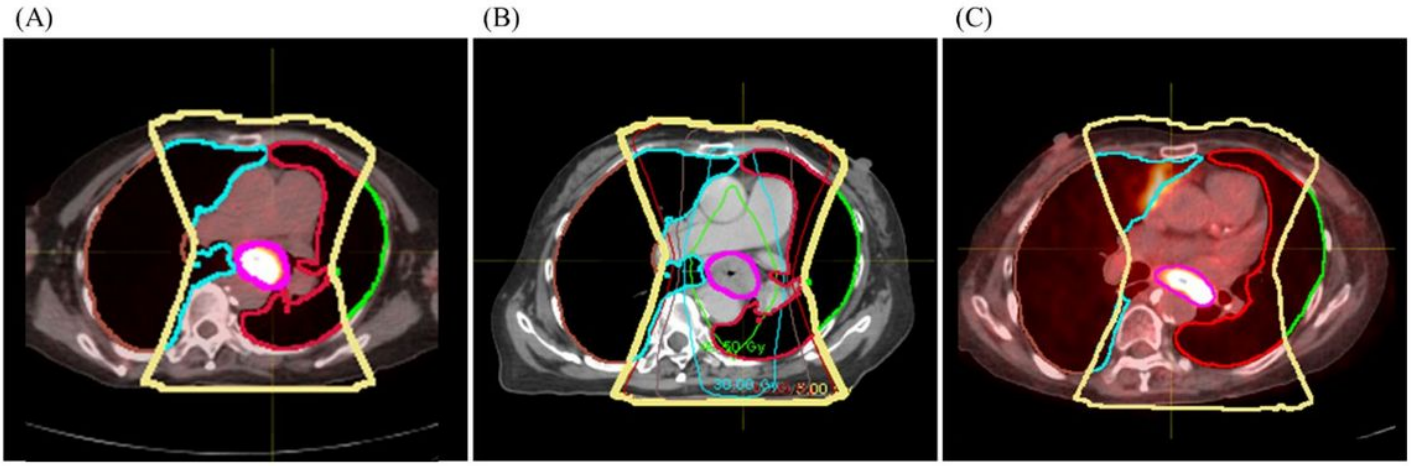

Figure 3

Comparison of area under the receiver operating characteristic curve of mean lung dose (MLD), lung V5, and lung V10 for discriminating the RP and nRP lungs.